AFWAL-TR-81-4019
Volume II

Scanning Electrode Techniques in Corrosion*

H. S. Isaacs and B. Vyas

Brookhaven National Laboratory

Upton, New York 11973

July 1981

*Research carried out under the auspices of the United States Department of Energy under Contract No. EY-76-C-02-0016

TABLE OF CONTENTS

	Page
LIST OF FIGURES	ii
ABSTRACT	iv
INTRODUCTION	1
EXPERIMENTAL TECHNIQUE	3
APPLICATIONS	4
Pitting Corrosion	4
Intergranular Corrosion	6
Welds	8
Stress Corrosion Cracking	9
SUMMARY	10
TABLE 1	11
REFERENCES	12

LIST OF FIGURES

FIG. 1 Schematic drawing of a local corrosion cell, showing (a) current paths in the electrolyte flowing from the anode to the cathode, and (b) equipotential lines in the electrolyte.....

FIG. 2 Schematic of the scanning reference electrode technique for flat samples (Ref. 13).....

FIG. 3 Schematic of the scanning reference electrode technique for a cylindrical rotating sample (Ref. 15).....

FIG. 4 Potential scans above an electropolished Type 304SS surface in 0.4M $FeCl_3$. The "period" after exposure to the electrolyte are shown (Ref. 19).....

FIG. 5 Potential scan of the boundaries attacked on a large grain size Type 304SS held at -200mV in 2.5N H_2SO_4 (a) area scan of the potential fields measured by the SRET, (b) line drawing of the boundaries etched on metallographic observation of the sample (dark lines). Also drawn are the lines across the peaks in Fig. (12a) (a) (dotted lines).....

FIG. 6 Anodic polarization for the large grain size Type 304SS in 2.5N H_2SO_4. Also shown are potential zones over which the material is susceptible to intergranular attack.....

FIG. 7 Polarization curve for Type 304SS weldment showing the potential regions over which the different types of preferential attack occur.....

LIST OF FIGURES (Cont'd)

FIG. 8 Potential scan across a propagating stress corrosion crack in Type 304SS exposed to LiCl at 90°C at a stress of 8.5Ksi. The crack is shown in the micrograph.....

FIG. 9 Potential profiles along the stress corrosion crack at various stages of the propagation in Type 304SS exposed to LiCl at 90°C at 8.5Ksi.....

Scanning Electrode Techniques in Corrosion*

H. S. Isaacs and B. Vyas

Brookhaven National Laboratory

Upton, New York 11973

ABSTRACT

The principles, advantages, and implementations of scanning reference electrode techniques are reviewed. Data related to pitting, intergranular corrosion, welds and stress corrosion cracking are presented. The technique locates the position of localized corrosion and can be used to monitor the development of corrosion and changes in the corrosion rate under a wide range of conditions.

*Research carried out under the auspices of the United States Department of Energy.

INTRODUCTION

The definition of localized corrosion usually is restricted to specific types of attack often related to the presence of chlorides. This definition may be broadened to incorporate all other cases where corrosion takes place at specific areas of the metal surface. General corrosion rates in most systems have been measured and design allowance can be made for the metal losses during the expected life of the system. Problems arise when the corrosion becomes localized and the penetration rate of the metal is orders of magnitude greater than the predicted general corrosion. Localized forms of corrosion, therefore, take a far greater toll than the incorrect choice of materials having unacceptable general corrosion rates.

During localized corrosion,[1,2] the electrochemical dissolution is well separated from the cathodic reactions. This makes an *in situ* study of the anodic and cathodic reactions amenable to direct measurement and to clearly separate the anodic and cathodic reactions in contrast to general corrosion where the reactions can take place in close proximity. *In situ* measurements such as mapping of potentials in solution or the physical separation of anodic and cathodic areas and measuring the currents flowing between them have been used successfully to identify the processes during corrosion.[3,16]

Figure 1 shows a schematic of the flow of current in the electrolyte from a localized anodic to the surrounding cathodic areas and equipotentials set up around the localized electrode. By scanning a "passive" reference probe with a fine capillary tip parallel and in close proximity to the metal surface the potential distribution in the liquid can be measured. The potential changes are most rapid over the localized electrode and a potential maximum or minimum is observed over its center. In the SRET work presented here, the sign convention

adopted is opposite to that generally used in order to show anodic areas as potential peaks and cathodic areas as minima. Thus, the SRET is an in situ technique to locate the anodic and cathodic sites and study the electrochemical processes during localized corrosion, without altering the processes taking place, changing the local environment over the corrosion site or influencing the rate of corrosion. The scanning technique has been recently reviewed.[11]

Areas around a weld have been studied separately using a liquid drop drawn across the sample. The potential variations and the polarization characteristics as a function of the drop position were measured.[3] In another study,[4] an insulating coating over a weld area was perforated with a micro-hardness indentor, and a liquid drop was placed over the perforation and the potential and the polarization characteristics of the underlying deformed metal was determined.

The flow of current from the anodic to the cathodic areas can also be determined without sectioning samples. In an early work on water line corrosion, Evans and Agar[5] calculated the current from the measured equipotential lines during the corrosion of zinc. A scanning reference electrode technique (SRET) was used to measure the potential variation in the solution. An agreement of within 10% was obtained between the measured corrosion rates from weight loss and the calculations from the equipotential surfaces.

Jaenicke and Bonhoeffer,[6,7] Copson[8] and Rozenfeld[9] measured the potential distribution around galvanic couples and calculated the corrosion rates and the surface current density distributions. Measurements of potential distribution during corrosion of bismuth-cadmium and zinc-aluminum alloys were also studied.[7] More recent measurements of couples of iron and copper have been conducted by Heldebrand and Schwenk.[10]

EXPERIMENTAL TECHNIQUE

The potential fields generated in the electrolyte due to local corrosion sites can be measured by scanning a microtip reference electrode over a horizontal exposed surface facing up. The equipment built at Brookhaven National Laboratory is shown schematically in Fig. 2.[12,13] The microtip reference electrode is held by a mechanical stage attached to low friction, linear bearings for smooth motion in the X and Y direction, and driven by two stepping motors. The mechanical stage can be automatically programmed to scan both in the X and Y directions parallel to the specimen surface. The length of the X direction can be varied up to 26 mm, and, at each end of the X scan, the Y direction can be shifted to a set value (from 30 m to 200 m). Thus, an area of the surface is scanned by a rectangular wave. The linear speed of the scan in the X direction can be varied from 0.1 mm/sec to 300 mm/sec.

Alternatively, potential fields on cylindrical samples can be obtained by keeping the probe stationary while rotating the sample.[14,15] The microtip reference electrode measures the potential variations along the circumference of the sample as the potential field around the sample rotates with the sample. A schematic of such an instrument is shown in Fig. 3.[15] A motor is used to rotate a cylindrical metal specimen in the electrolyte such that the rotational motion of the sample is synchronized to produce a signal which is proportional to the angular position of the sample with respect to the probe. The microtip reference electrode is made to scan in the vertical direction (parallel to the cylindrical axis). If the signal of the sample rotation is fed to the X direction and signal of scan of the probe to the Y direction, the surface scan of the cylindrical specimen is obtained. The size of the area examined on the specimen surface can be controlled by regulating the length over which the microtip refer-

ence electrode moves along the axis of the sample and controlling the time per revolution of the specimen.

The potential field in the electrolyte during localized corrosion is the difference in the potential measured by the microtip reference electrode and a reference electrode placed more than 10 mm away from the sample surface. The two signals are fed into a differential electrometer and the resultant potential amplified to the desired amount. The potential fields can be plotted on a X-Y recorder by feeding the signal from the X position of the motor to the X amplifier of the recorder the sum of the Y position of the motor and the amplified potential difference to the Y amplifier of the recorder. Thus, one obtains a two dimensional plot of the potential field variations at a plane parallel to the sample surface. The signals can also be recorded on a storage oscilloscope and photographed. Alternately, the amplified potential difference can modulate the intensity of the cathode ray tube of an oscilloscope,[11] or plot the equipotential lines from an analyzer.[15]

APPLICATIONS

Pitting Corrosion

Pitting corrosion is a highly localized form of corrosion attack of passive metal surfaces and is generally directly related to the presence of chlorides or bromides. The development of pitting is sensitive to almost all variables associated with the interface between the metal and the electrolyte. These variables include the chloride concentration, the presence of other anions which may act as pitting inhibitors, the composition of the metal, its surface preparation and history and the electrochemical potential.[16-22]

The pitting behavior of stainless steels was investigated by Rosenfeld and Danilov using the adjacent reference electrode technique.[16] Their measure-

ments were carried out in a solution containing about 0.05M $FeNH_4(SO_4)_2$ and 0.1 or 0.56M NH_4Cl. They could detect pits after 30-60 secs after contact with the solution. Initially the rates of dissolution of all the pits were similar, however, with time, some of the pits stopped corroding or showed decreased rates. Observations of the pits under the microscope showed that they were covered by a film or shielding layer resulting from the attack of the metal by chloride ions penetrating the oxide film. Destroying the shielding layer led to passivation. The authors considered the rupture of the shield assisted the diffusion of the "passivator" into the pit. The process of passivation took a relatively long time, of the order of tens of minutes, after disruption of the shield. Also, the time for deactivation of the pits increased with the size of the pits.

The currents from the pit were related to the square root of time. The current densities, therefore, decreased and assuming a hemispherical pit, the surface area varied linearily with time. This result is in agreement with work by other investigators.[17,18]

The SRET has been used to study the pitting of type 304 stainless steels in a ferric chloride solution[12,21] composed of 0.4M $FeCl_3$ and adjusted to pH 0.9.[20] The change in the number of active pits were studied as a function of time and surface preparation. On exposing the steel to the solution, the potential of the specimen increased rapidly above the pitting potential with the generation of active pits. With time, the potential of the specimen decreased as the active pits grew and the number decreased. However, small potential increase were observed when pits passivated. The active and repassivated pits were separated using the SRET. The active pits were always covered by a film and contained a dark green solution. Fig. 4 shows a sequence of scans

represented by potential surfaces for an electropolished surface at the times shown. Each peak is associated with the currents from active pits. On the first scan, initialed one minute after exposure, fourteen pits could be identified. The number of active pits decreased and only one pits was active after 26 minutes. When the final pit was subjected to a jet of solution, it repassivated. The anodic currents polarizing the cathodic reaction then ceased and the potential rose rapidly above the pitting potential and the sequence of events observed on first contacting the specimen with the chloride solution was repeated.

It was suggested that the film over the active pits was the passive oxide film originally on the metal surface that was undermined by the pitting process.[12] This possible explanation was investigated by varying the surface preparation of the stainless steel prior to pitting.

The results were found to be consistent with the changes in the properties of the original oxide layer over the pit before it was undermined by the pitting process. The thicker the oxide, the greater was the protection afforded to the growing pit and the longer the pits remained active. When the metal was abraded, stresses in the oxide film lead to short half-lives (< 1 sec). The half-lives of pits on abraded surfaces was low (~ 5 min.) even after oxidation at 250°C in comparison to similarly oxidized electropolished surfaces which gave a half-life of 480 minutes.

Intergranular Corrosion

Intergranular corrosion (IC) is defined as the localized attack, at the grain boundaries of steels. This form of corrosion is particularly severe in stainless steels which are sensitized. Sensitization is caused by (1) heat treating the alloy in the temperature range of 500-850°C for a few hours and

quenching; (2) cooling slowly through the above mentioned temperature range and; (3) welding.[23,24] It is generally believed that sensitization leads to the precipitation of chromium rich carbides at the grain boundaries and the depletion of chromium adjacent to the boundary.[25] This depletion has been observed by scanning transmission electron microscopy.[26] The depletion of chromium at the grain boundary leads to IC of stainless steels in certain environments.

The SRET has been used to determine the accelerated corrosion of grain boundary region in sensitized type 304 stainless steel. Fig. 5(A) is a potential scan during the IC of a large grain size (diameter ~ 3 mm), sensitized (600°C for 24 h) type 304 stainless steel in 2.5N H_2SO_4 at room temperature at a potential of -200 mV vs. SCE. Fig. 5(B) is a line drawing of the etched boundaries on metallographic observation after the test showing a clear relation between the etched boundaries (dark lines) and the peak maximum in Fig. 5(B) (dotted lines). The potential peaks were observed only in the case of sensitized type 304 stainless steel, while solution annealed (1100°C for 3 hrs) samples exhibited no peaks and no grain boundary etching in this solution.

The dependence of intergranular corrosion on the electrochemical potential of type 304SS in 2.5N H_2SO_4 can be determined by slowly increasing the potential (0.3 V/h) of the sample in the anodic direction and scanning the surface simultaneously. In the potential region where sensitized type 304SS is susceptible to IC, peaks are observed on scanning, while in the potential region, where the material does not undergo IC no peaks are observed. The material is susceptible to IC between -280 mV to +80 mV vs. SCE and then again in the transpassive region (> 820 mV vs. SCE), as shown in Fig. 6. This result is consistent with the observation of IC of this steel in the Strauss test and the nitric acid test.[27]

Welds

In welding, it is assumed that corrosion behavior of the weld metal and the parent metal is similar. However, this is not always the case, particularly when austenitic stainless steels are considered. The weldment, i.e. the weld metal and the adjacent parent metal affected by the heat of the welding, may be susceptible to varying degrees of preferential attack. The weld metal may corrode more or less than the parent metal due to differences in composition or metallurgical condition.[24] In addition, the base metal heated during the welding may corrode as a result of metallurgical changes caused by heating cycles.[23] The factors that can influence the type and degree of preferential attack depend on 1) composition and structure of base and weld metal, 2) metallurgical changes in the parent metal due to welding, 3) welding process and procedure, 4) size of material welded, and 5) the type of the environment.[28]

The SRET has been successfully used to identify the preferential attack of type 304 stainless steel weldments. The type of preferential attack observed are 1) attack of the ferrite in the weld matrix, 2) fusion boundary corrosion, 3) intergranular corrosion of the sensitized material in the heat-affected zone of the base metal.[13] A type 304 stainless steel weldment was tested in 2.5N H_2SO_4 at room temperature at various potentials. The potential regions exhibiting the different types of preferential attacks are shown in Fig. 7.

Sensitization in the heat affected zone adjacent to the weld is probably the most common cause of intergranular corrosion and intergranular stress corrosion cracking in stainless steels in service. In order to determine the susceptibility of a given weldment to these forms of localized attack, it is necessary to develop a test which will give 1) the location of the sensitized zone, and 2) a quantitative measure of the degree of sensitization. The SRET meets the above

mentioned requirements and has been successfully used to give the location and the degree of sensitization of the weldments for various welding process variables. The details of the test are given in detail elsewhere.[13]

Stress Corrosion Cracking

Stress corrosion cracking in metal systems is concerned with the nucleation and propagation of cracks in stressed metals induced by the environment. In order to understand the mechanism of cracking in any particular metal-environment system, it is necessary to determine the electrochemical reaction(s) that take place at the crack tip. The SRET provides an ideal system to study this reaction and in this section, an example is given of SCC of type 304 stainless steel in a chloride solution. The electrolyte used was 20 molal LiCl controlled at 90°C.

Fig. 8 shows the potential peaks observed after the cracking had progressed into the metal. The propagation of the potential peaks was studied. Fig. 9 gives the magnitude of potential peaks along the length of the crack at various times taken from figures similar to Fig. 8. The shape of these plots which are non-symmetrical, indicates that although the dissolution rate was greatest at the crack tip, the entire crack remained active. These observations are consistent with most theories of stress corrosion cracking, i.e. rapid dissolution takes place at the high stress intensity at the crack tip where fresh metal is continuously exposed to the corrosive environment.[29] However, the persistent anodic dissolution of the crack surfaces shown using SRET, during cracking and after the specimens fail, is in conflict with models which suggest that the crack surface must passivate to account for crack propagation. The SRET suggests that the exposed metal remains active but with decreased dissolution rates.

SUMMARY

The SRET has been shown to offer a technique for studying localized forms of corrosion including pitting, intergranular corrosion and stress corrosion cracking. These processes are associated with relatively rapid dissolution rates and observable potential variation in solution. The technique is also useful in separating preferential dissolution or cathodic reactions under controlled potentials where external currents flow.

Other electrochemical measurements e.g. polarization techniques, can give detailed information about processes under study, but, difficulties arise in the complete separation of the anodic and cathodic areas and duplicating the conditions operative during corrosion. The SRET overcomes these difficulties, and offers an approach for *in situ* determination of the corrosion processes and allows for clarification of the factors involved, without extraneous effects influencing the corrosion.

TABLE 1. Variations of Pit Half-Life with Surface Preparation

Surface treatment	Pit half-life,* min
Electropolished and cathodically polarized	<1
As electropolished	22
Electropolished and oxidized at 110°C for 24 hr	90
Electropolished and oxidized at 165°C for 24 hr	150
Electropolished and oxidized at 240°C for 24 hr	430
Electropolished and oxidized at 250°C for 2 hr	480
Electropolished and oxidized at 300°C for 22 hr	340
Electropolished and oxidized at 375°C for 2 hr	270
Abraded with 600 grade SiC	<1
Abraded and oxidized at 250°C for 8 hr	5

*Maximum variation of 20%

REFERENCES

1. Localized Corrosion - Cause of Metal Failure ASTM, STP 516, American Society of Testing & Materials, 1972.

2. Brown, B.F., Kruger, J. and Staehle, R.W., Eds., Localized Corrosion, National Association of Corrosion Engineers, 1974.

3. Lajain, H. Z.F. Werkstofftechnik, Vol. 2 (1971), p. 19.

4. Lajain, H. Werkstoffe und Korrosian, Vol. 23 (1972), p. 537.

5. Evans, U.R. and Agar, J.N., see Evans, U.R., The Corrosion and Oxidation of Metals, Edward Arnold Ltd., 1960, p. 862; Evans, U.R., Journal of the Iron and Steel Institute, I, Vol. 141, 1940, p. 219.

6. Jaenicke, W., Z. Physik Chem., Vol. A191, 1943, p. 350.

7. Jaenike, W. and Bonhoeffer, K.F., Z. Physik Chem., Vol. 193, 1944, p. 301.

8. Copson, H.R., Journal of the Electrochemical Society, Vol. 84, 1943, p. 71.

9. Rozenfeld, I.L. Atmospheric Corrosion of Metals, National Association of Corrosion Engineers, 1972, p. 83.

10. Hildebrand, H. and Schwenk, W., Werkstaffe und Korrosion, Vol. 23, 1972, p. 364.

11. Isaacs, H.S. and B. Vyas, Electrochemical Corrosion Testing ASTM, STP 727, F. Manfield and V. Bertocci, Eds., American Society for Testing and Materials, 1981, p. 3.

12. Isaacs, H.S., in Ref. 1, p. 158.

13. Vyas, B. and Isaacs, H.S., Intergranular Corrosion of Stainless Alloys, ASTM, STP 656, R.F. Steigerwald, Ed., American Society for Testing and Materials, 1978, p. 133.

14. Bhansali, J.J. and Hepworth, M.T., Journal of Physics E. Scientific Instruments, Vol. 7, 1974, p. 681.

15. Gainer, L.J. and Wallwork, G.R., Corrosion, Vol. 35, 1979, p. 61.

16. Rosenfeld, I.L. and Danilov, I.S., Corrosion Science, Vol. 7, 1967, p. 129.

17. Engell, H.J. and Stolica, N.D., Z. Phys. Chem., Vol. 20, 1959, p. 113.

18. Sato, N., Nakagawa, T., Kudo, K. and Sakashita, M.S. in Ref. 1, p. 447.

19. Isaacs, H.S. and Kissel, G., Journal of the Electrochemical Society, Vol. 119, 1972, p. 1628.

20. Wilde, B.E. and Williams, E., Journal of the Electrochemical Society, Vol. 117, 1970, p. 775.

21. Galvele, J.R., in Passivity of Metals, R.P. Frankenthal and J. Kruger, Eds., The Electrochemical Society Inc., 1978, p. 285.

22. Wilde, B.E. and Williams, E., Electrochimica Acta, Vol. 16, 1971, p. 1971.

23. Cowan, R.L. and Tedmon, Jr., C.S., Advances in Corrosion Science and Technology, Vol. 3, 1973, p. 293.

24. Henthorne, M., Localized Corrosion - Cause of Metal Failure, ASTM, STP 516, 1972, p. 66.

25. Tedmon, Jr., C.S., Vermilyea, D.A. and Rosolowski, J.H., J. Electrochem. Soc., Vol. 118, 1971, p. 192.

26. Pande, C.S., Suenaga, M., Vyas, B., Isaacs, H.S., and Harring, D.F., Scripta Met., Vol. 11, 1977, p. 601.

27. ASTM Designation, Recommended Practice for Detecting Susceptibility to Intergranular Attack in Stainless Steel, 1970.

28. Clarke, W.L., Cowan, R.L. and Walker, W.L., Intergranular Corrosion of Stainless Alloys, ASTM, STP 656, R.F. Steigerwald, Ed., American Society for Testing and Materials, 1978, p. 99.

29. Latanision, R.M. and Staehle, R.W., in Fundamental Aspects of Stress Corrosion Cracking, R.W. Staehle, A.J. Forty and D. van Rooyen, Eds., National Association of Corrosion Engineers, 1969, p. 278.

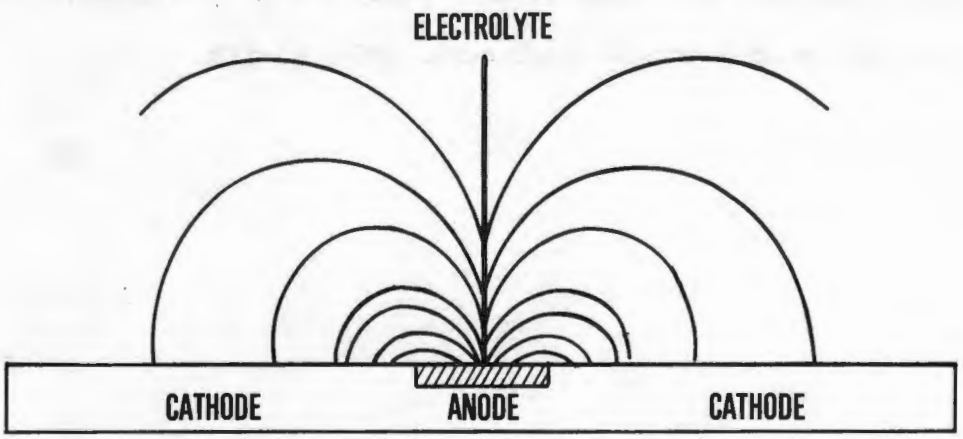
ELECTROLYTE
CATHODE
ANODE
CATHODE

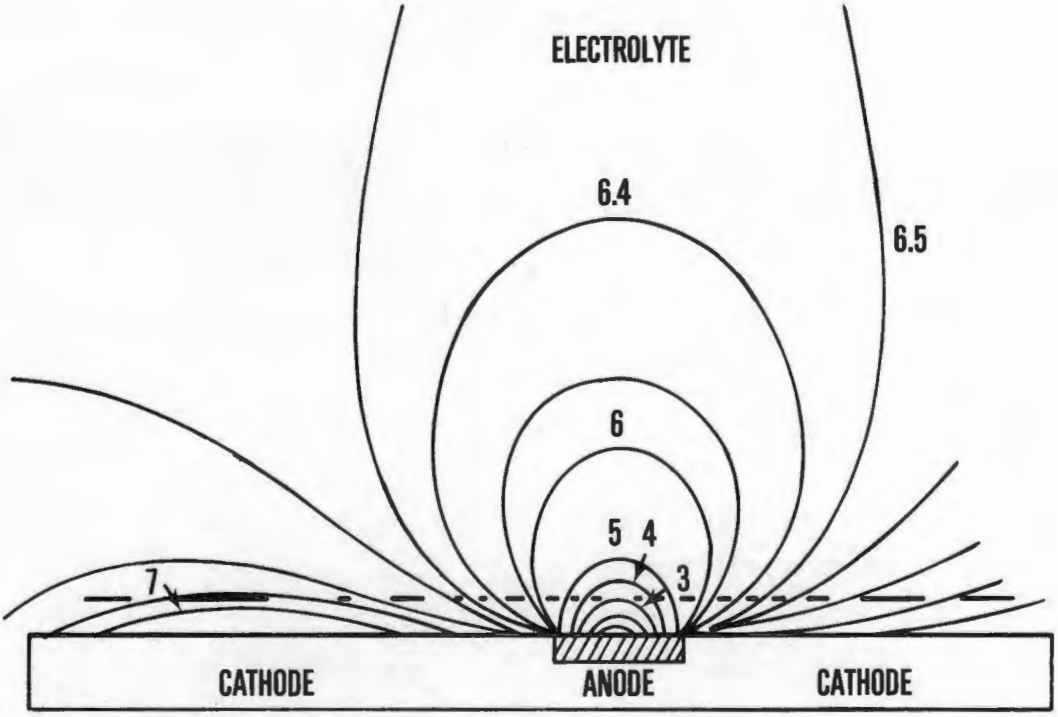
ELECTROLYTE
6.4
6.5
6
5
4
3
7
CATHODE
ANODE
CATHODE

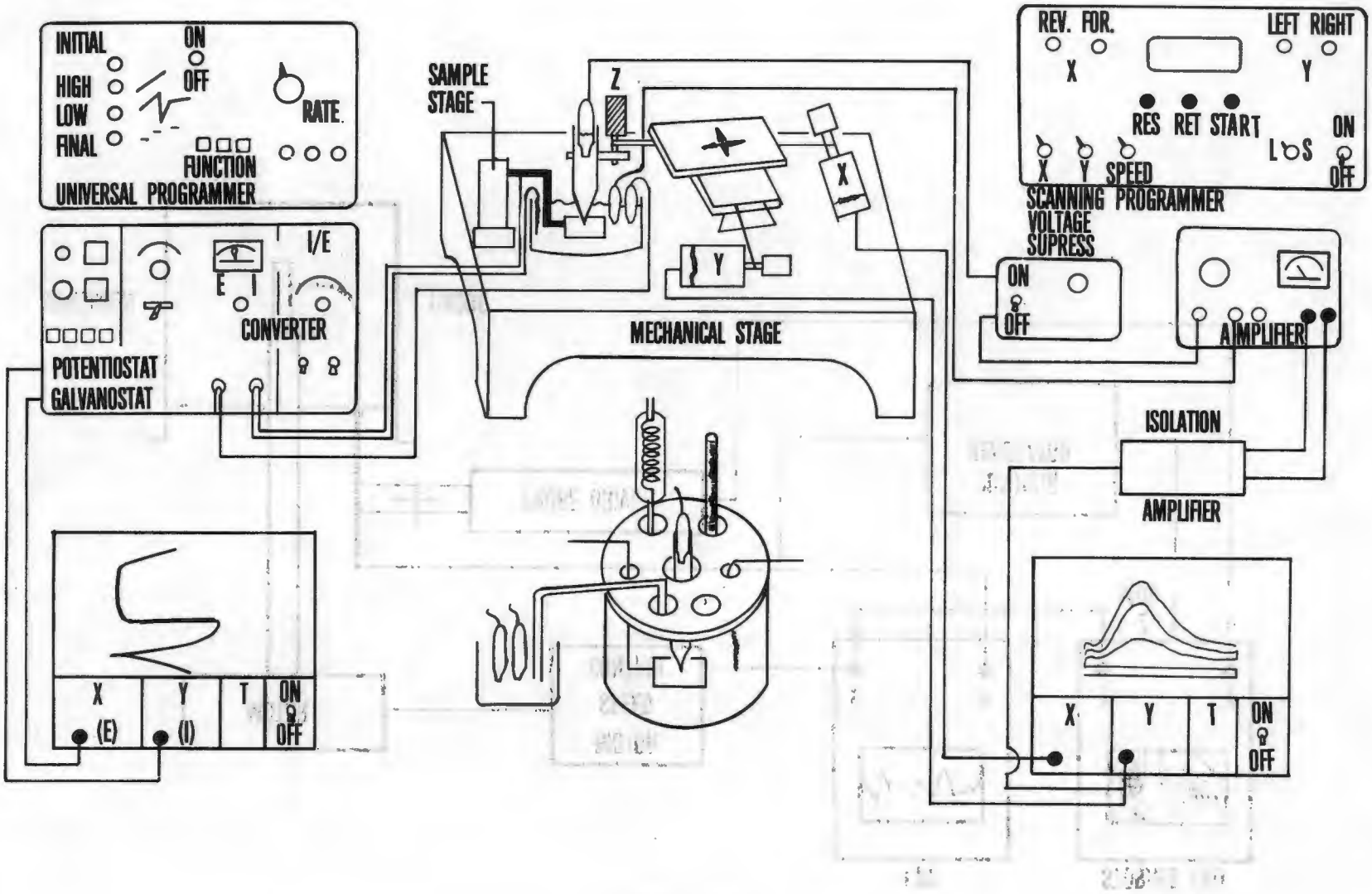
INITIAL
ON
HIGH
OFF
LOW
RATE.
FINAL
FUNCTION
UNIVERSAL PROGRAMMER
I/E
E
I
CONVERTER
POTENTIOSTAT
GALVANOSTAT
SAMPLE
STAGE
Z
X
Y
MECHANICAL STAGE
REV. FOR.
LEFT RIGHT
X
Y
RES RET START
ON
OFF
X Y SPEED
SCANNING PROGRAMMER
VOLTAGE
SUPRESS
ON
OFF
AMPLIFIER
ISOLATION
AMPLIFIER
X
Y
T
ON
OFF
(E)
(I)

Figure 2

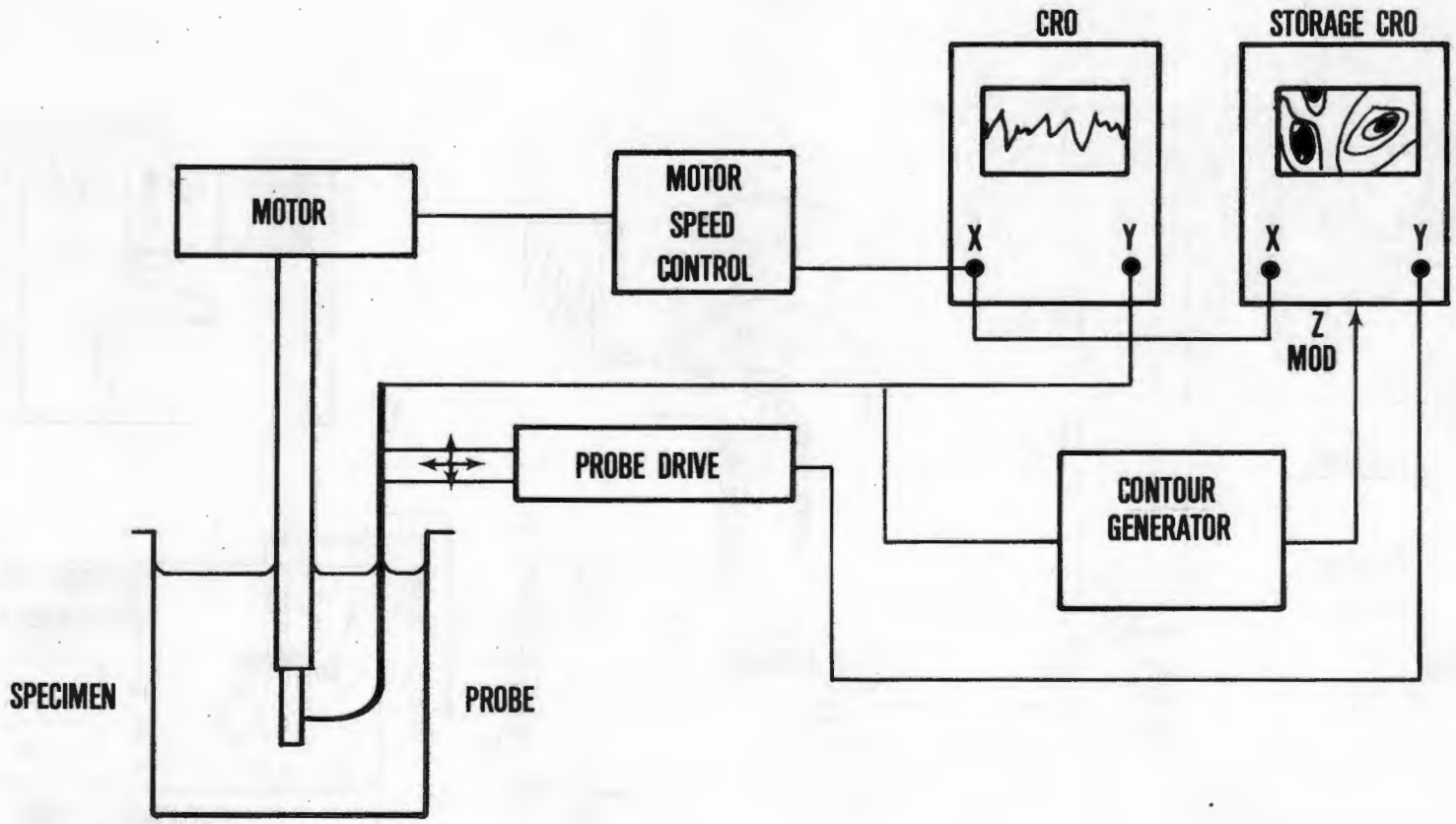
CRO
STORAGE CRO
MOTOR
MOTOR SPEED CONTROL
X
Y
X
Y
Z MOD
PROBE DRIVE
CONTOUR GENERATOR
SPECIMEN
PROBE

Figure 3

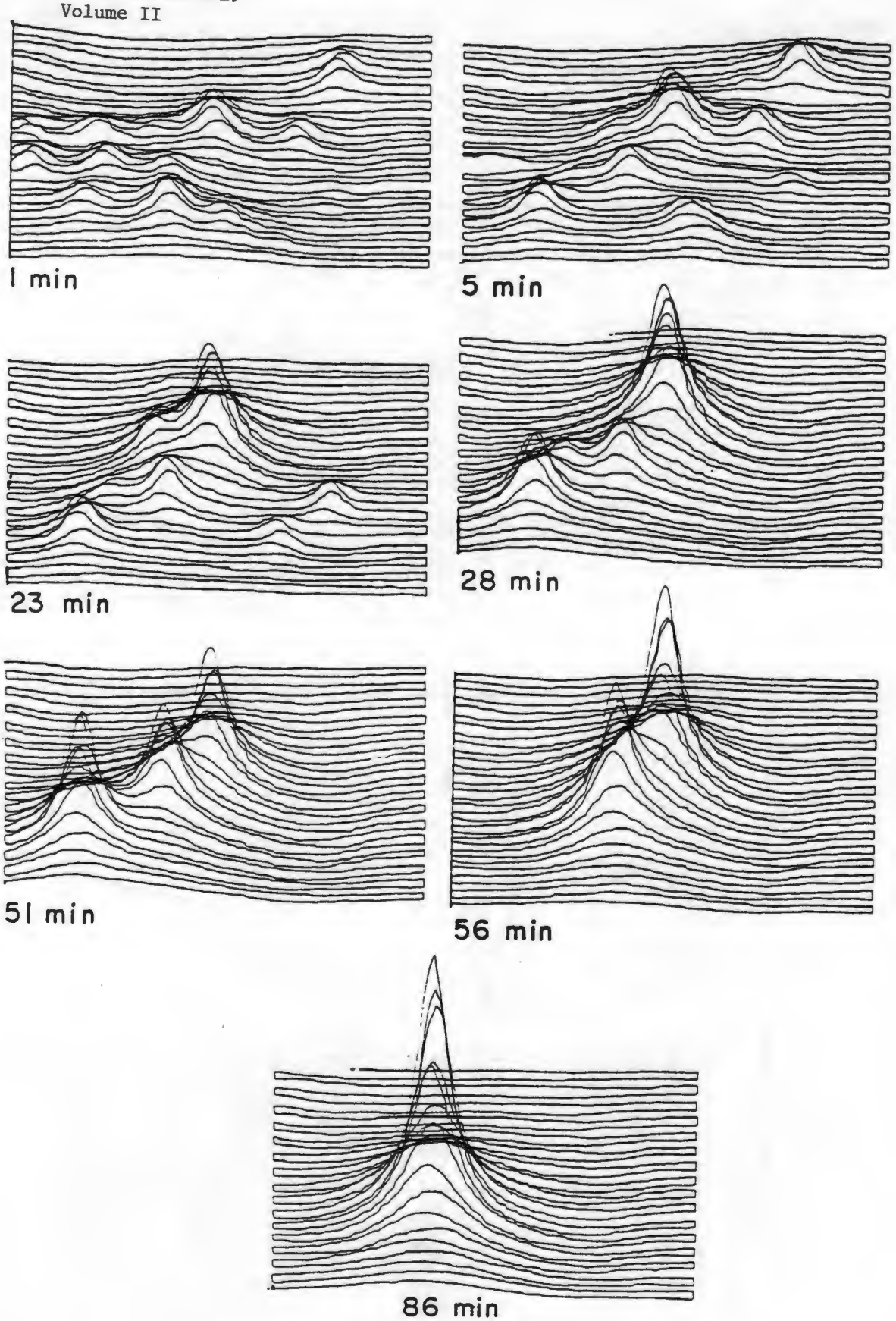

Figure 4

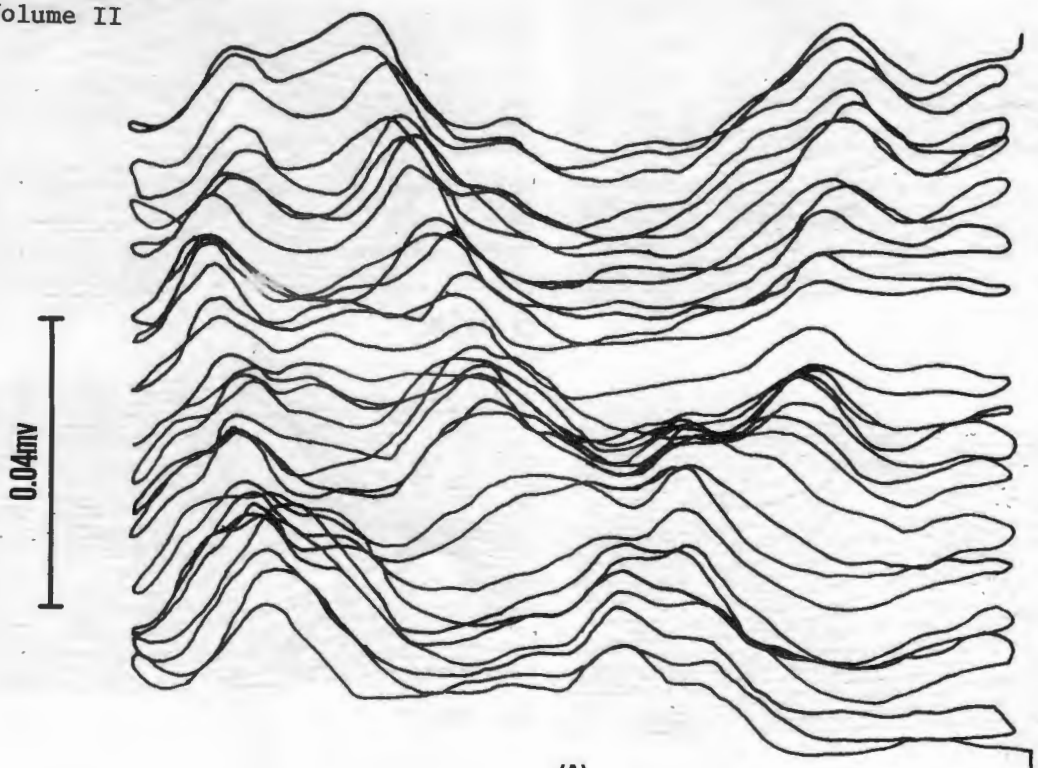

(A)

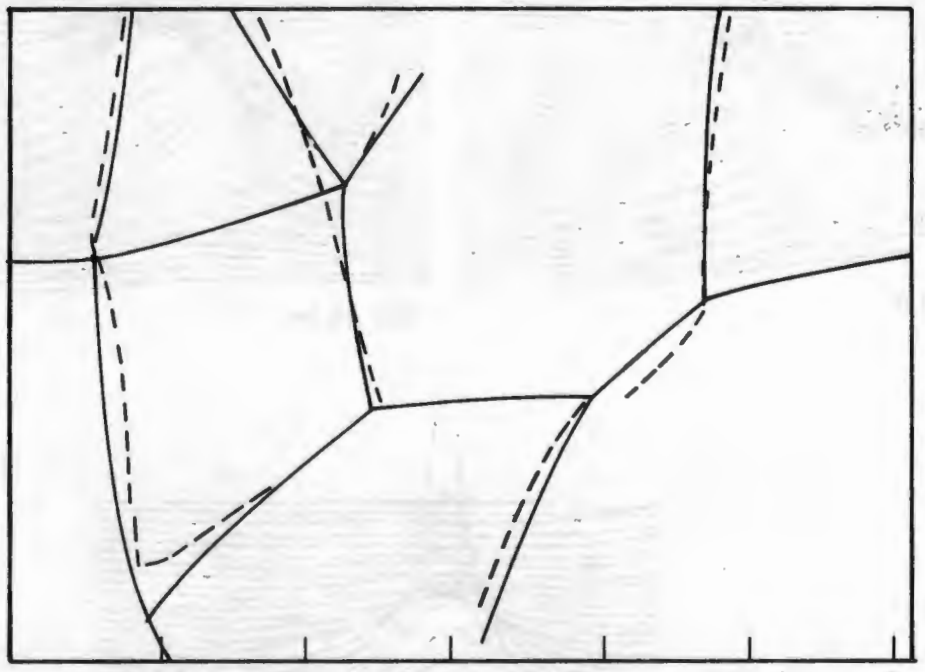

(B)

Figure 5

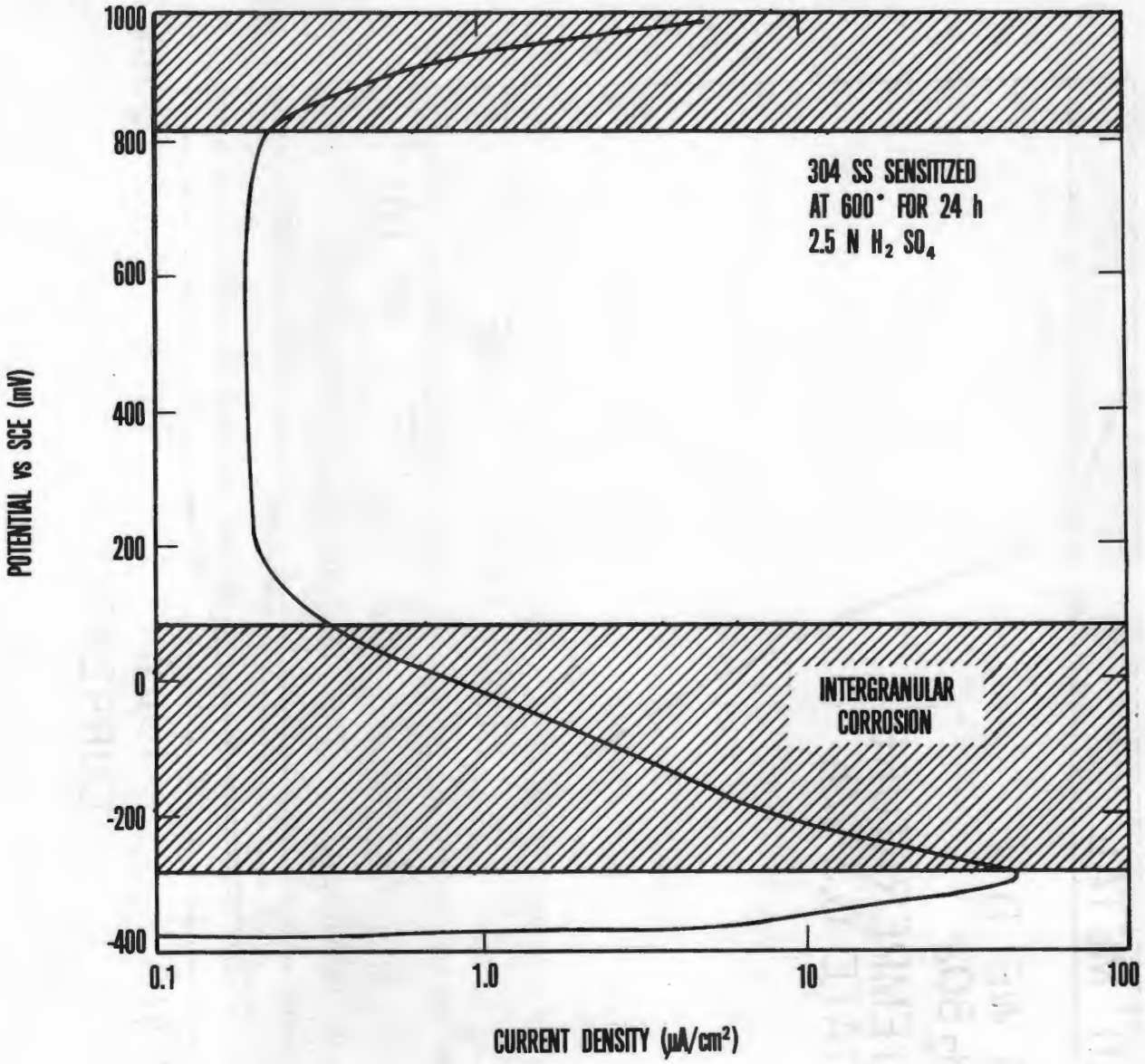
1000
800
600
400
200
0
-200
-400
POTENTIAL vs SCE (mV)
304 SS SENSITIZED
AT 600° FOR 24 h
2.5 N H_2SO_4
INTERGRANULAR
CORROSION
0.1
1.0
10
100
CURRENT DENSITY (μA/cm²)

Figure 6

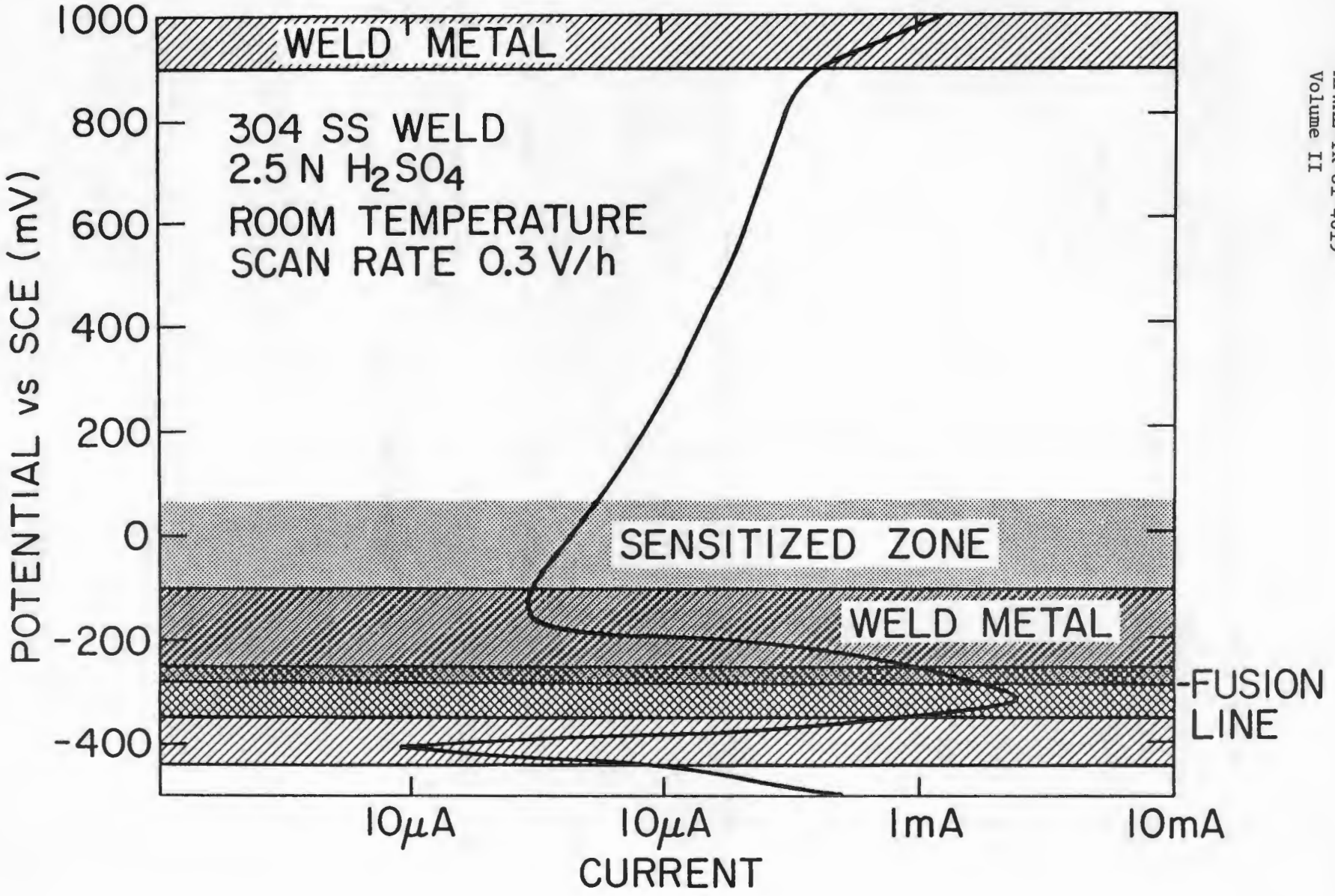
1000
800
600
400
200
0
-200
-400
POTENTIAL vs SCE (mV)
WELD METAL
304 SS WELD
2.5 N H_2SO_4
ROOM TEMPERATURE
SCAN RATE 0.3 V/h
SENSITIZED ZONE
WELD METAL
FUSION LINE
10μA
10μA
1mA
10mA
CURRENT

Figure 7

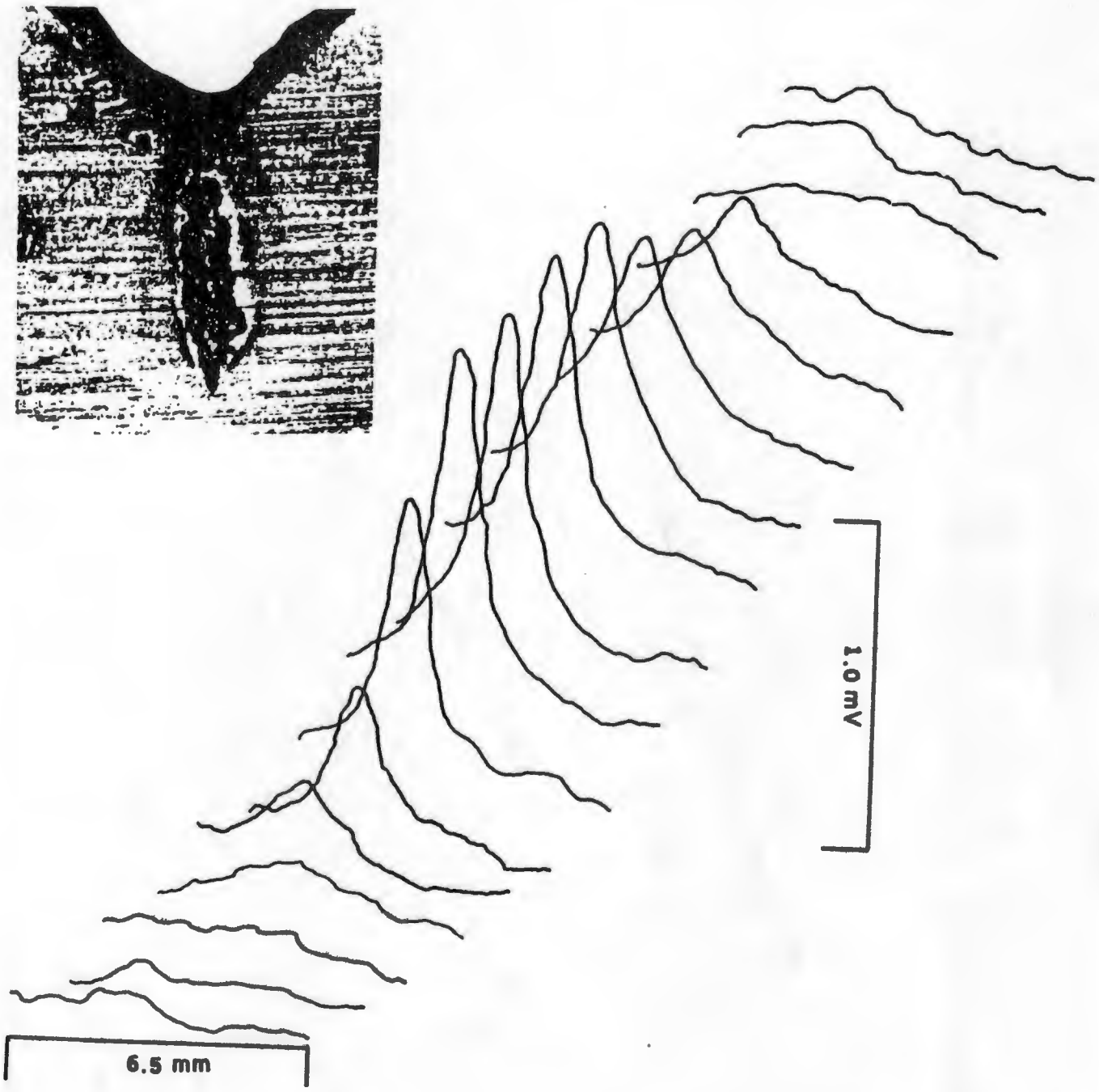

Figure 8

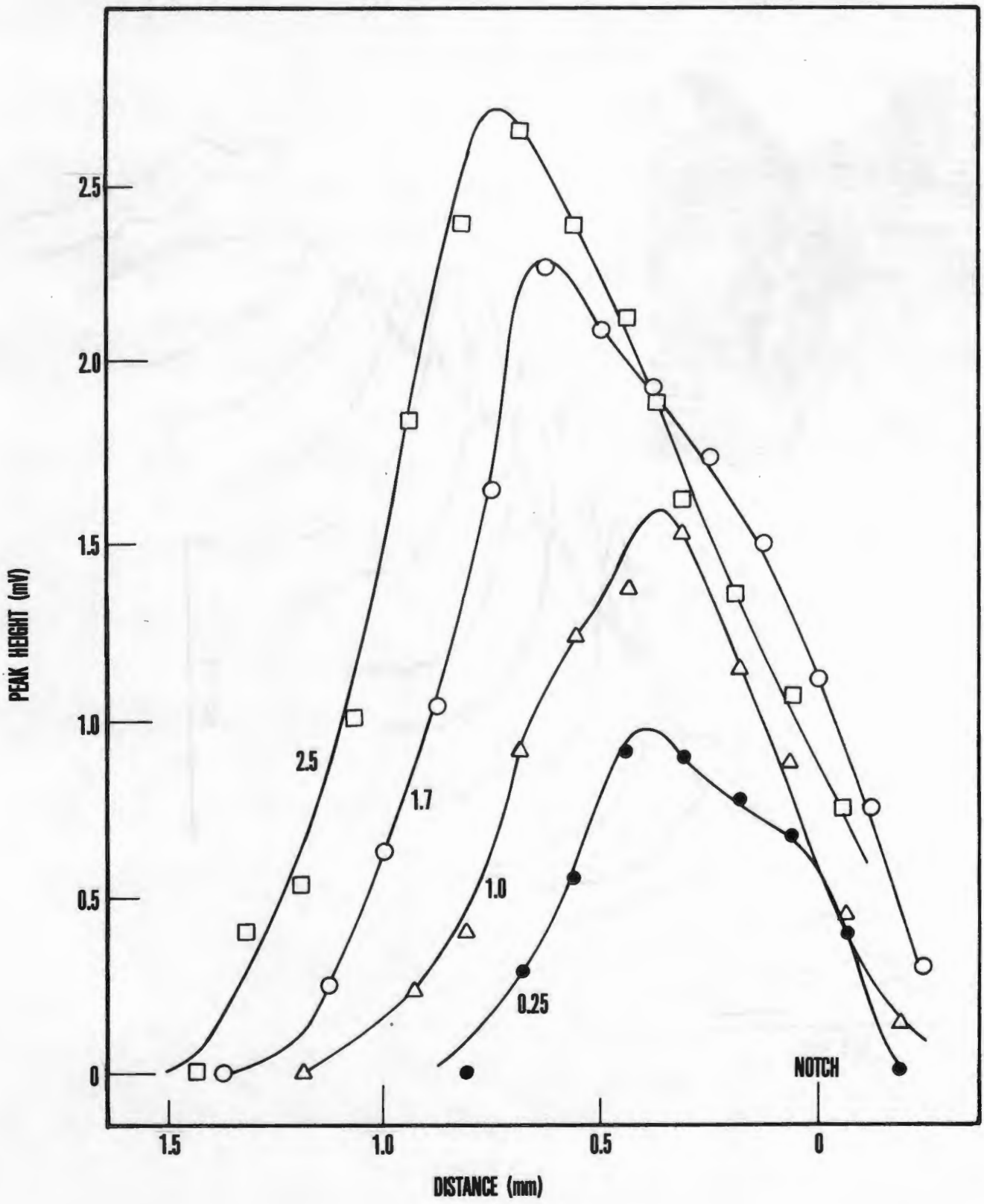
PEAK HEIGHT (mV)
2.5
2.0
1.5
1.0
0.5
0
2.5
1.7
1.0
0.25
NOTCH
1.5
1.0
0.5
0
DISTANCE (mm)

Figure 9